Analysis of a gaseous partially premixed lifted flame in swirling flow through different LES combustion models

L. Langone[*], D. Pampaloni, L. Mazzei, A. Andreini

[1]Departement of Industrial Engineering – University of Florence
via di S. Marta, 3, Florence, 50139, Italy

Abstract

The present study numerically investigates a low-swirl partially premixed lifted flame employing gaseous fuel through CFD calculations in Large Eddy Simulations (LES) context. Lifted flames have been studied in many different configurations during the last decades since their potential in terms of pollutant emissions and stability. Nevertheless, the stabilization mechanism behind this type of flame is still not completely understood. Two different combustion modeling strategies are adopted: the Flamelet Generated Manifold (FGM) approach and the Artificially Thickened Flame (ATF) model. Moreover, an extended version of the FGM model including stretch and heat loss effects is applied. Numerical results are compared with the available experimental data in terms of temperature and carbon monoxide concentration maps showing that the ATF model has a substantial advantage on the FGM concerning the description of the physics involved.

Introduction

In recent years, research in the gas turbine (GT) field has focused on the development of new combustion systems to guarantee both low emission and safe operability among all the possible loads and ambient conditions. A possible strategy could be represented by the use of partially premixed lean lifted flames, characterized by the main reaction zone considerably detached from the nozzle exit by a distance often called *lift-off height* (LOH) in the literature. This specific flame configuration brings some benefits, such as the improvement of the mixing between fuel and oxidizer before reaching the flame front concerning the classic partially premix burner concept. This fact allows to safely operate with a global lean equivalence ratio avoiding the use of pilot injectors. Also, the service life of the nozzle is increased, since it experiences lower operational temperatures. This concept of flame has been widely investigated in the literature concerning both academic test cases and industrial applications [1]. However, considering the GT application field, two main concepts have been proposed by Cheng [2], and Zarzalis [3], both employing a low-swirl injector. The latter concept is particularly interesting since it remains close to a currently adopted injector for industrial applications while showing promising results in terms of nitrogen oxides reduction. This injector has also demonstrated improved stability in terms of Lean Blow-Out (LBO) occurrence [4], [5], which potentially allows operating at even leaner load conditions. Even if several numerical and experimental studies have been conducted on lifted flames during the last decades, a clear understanding of the main stabilization mechanism is not reached. This fact is due to the many effects playing a role in the stabilization of the flame, without a unique mechanism taking over the others involved [1], [6]. Therefore, the development of proper modeling of the combustion process occurring in the combustion chamber is mandatory to allow further possible practical applications of lifted flames. The main point shared by all the studies so far carried out is that the finite rate effects revest a major role in flame stabilization and position. The lift-off region is characterized by mixing processes, ignition of the fresh mixture in contact with hot combustion products, and also local quenching phenomena. Considering the mentioned low-swirl concept, as far as the authors are aware, only a few numerical works have been carried out on this type of combustion chamber, namely by Kern et al. [7] and Sedlmaier [8]. The results are showing a misprediction of the flame position and shape, again highlighting the challenges of the numerical modeling for this type of flame. Considering this, the present work aims to understand the limitations of two of the most diffused combustion model within LES simulation for GT applications, the Flamelet Generated Manifold (FGM) and the Artificially Thickened Flame (ATF) models. This work follows a previous numerical study performed by the authors on a gaseous flame with a downscaled version of the same injector concept, where the FGM approach and a modified version of this combustion model were applied. The outcomes have shown that, although the lift-off occurrence was reproduced, the flame shape and extension were not completely in agreement with the experimental measurements. Another important finding was represented by the improvement reached by introducing the effects of local quenching phenomena through the modified version of the FGM approach. Here the goal is to furtherly evaluate these two approaches considering chemical species concentrations, other than verifying the impact of the a priori assumptions on the combustion regime (i.e., flamelet regime) with a different combustion model such as the ATF.

Test Case

The test case here considered is a gaseous lifted flame in a confined configuration investigated by Fokaides at the Engler-Bunte Institut of the Karlsruhe Institute of Technology (KIT-EBI) [4], [9]. The test rig consists of a cylindrical combustion chamber that can operate with both gaseous and liquid fuel: a sketch of the test rig with the low-swirl nozzle concept is present in Figure 1.

The main combustion chamber consists of a ceramic segment with water cooling. The test point considered in the present work employs methane as fuel and the associated operating conditions are reported in Table 1.
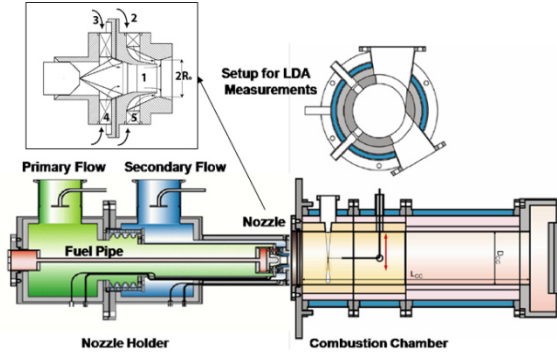
Figure 1 - Experimental test rig and low-swirl nozzle concept investigated by Fokaides [9].

Table 1 - Lifted flame experiment operating conditions.

Operating pressure	101325 Pa
Air inlet temperature	373 K
Air mass flow	0.0185 kg/s
Δp/p nozzle	2%
Equivalence ratio	0.65

The key feature of this burner is a radial double-swirl nozzle [10] characterized by an overall theoretical swirl number $S_{th,o}$ below 0.4, where this number is defined as:

$$S_{th,o} = \frac{\dot{D}_i}{R_i \dot{I}_i}$$

being $\dot{D}_i$ the angular momentum flux, R_i the inner radius of the prefilmer lip at the smallest section and $\dot{I}_i$ the axial momentum flux. The injector is derived from an air-blast atomizer [10] and it is composed of a primary swirl with $S_{th,inner} = 0.76$ and a secondary swirl with a set of fully radial channels ($S_{th,outer} \approx 0.0$). The final result is a high-velocity swirling jet issuing from the nozzle, where the Inner Recirculation Zone (IRZ) is weak and enveloped within the high-velocity jet streams. A strong Outer Recirculation Zone (ORZ) is instead present due to the interaction between the chamber walls and the swirling jet. This zone has a relevant extension in the combustion chamber and plays a major role in the transport of hot combustion products from the main reaction zone to the base of the flame. This fact represents the main stabilization mechanisms according to the previous studies and the flame cannot be ignited without the confinement walls [9]. Experimental data are available for both flow-field in isothermal conditions as well as gas multi-species concentrations in the field with the reactive test points.

Numerical setup
The LES simulations employ the spatially-filtered compressible Navier-Stokes equations solved with the ANSYS Fluent 2019-R1 CFD suite [11]. Second-order schemes have been employed for both spatial and temporal discretization and the subgrid stress tensor has been modeled with the Dynamic Smagorinsky-Lilly model [12]. The numerical domain has been derived from a previous numerical study conducted by the authors [13] on an injector with the same features as the one introduced previously, but with a lower effective area. It includes all the combustion chamber, comprehensive of the nozzle and the air plenum placed upstream of it. The outlet is modeled as a convergent section to mimic the experimental setup. In the same work, both isothermal and reactive conditions are investigated, obtaining a good agreement with the available experimental data regarding the flow-field description in cold conditions. For this reason, in the present work, calculations have been focused on the reactive point to assess the differences between each adopted combustion model, assuming that the numerical model can correctly represent the flow structures in absence of reaction. The final mesh grid is composed of 16 million polyhedral elements, which have shown as the best setup in terms of both accuracy and computational efforts. The finer mesh grid is adopted within the swirler and in the flame tube up to 260 mm and reached the flame tube walls for the region where direct interaction with the flame is expected. The air mass-flow is imposed to the inlet boundary while the atmospheric pressure is set to the outlet one. The fuel is instead injected with a dedicated inlet upstream the prefilmer lip, accordingly to the experimental rig. No-slip condition is applied to the combustion chamber walls, while a temperature of 1000 K is imposed as thermal boundary condition according to previous numerical works on this test case [10] for the ATF model simulation. Instead, aiming to maximize the effect of the heat loss correction, a temperature of 700 K is applied for the FGM approach. Since no accurate information is available concerning the wall temperature and considering the relevant effects of the heat losses in the flame lift-off [13], this choice wants to clarify that potential misprediction related to the FGM is not related to improper boundary conditions, but an actual limit of this type of modeling. The time step has been set to 1e-06s, with a maximum value of the CFL below 5. The simulated physical time is 150ms corresponding to roughly 5 Flow Through Times of the combustion chamber.

Combustion modeling
As mentioned, three different combustion models have been adopted: the FGM model, a derived approach that takes into account the stretch and heat loss effects on the flame front here reported as Flamelet Generated Manifold Extended (FGM-EXT), and the ATF model. The FGM approach [14] assumes a flamelet combustion regime, where the flame front is only wrinkled by the turbulence but it could be described by laminar 1D flames. Therefore, it is possible to compute a priori a look-up table to describe all the thermochemical states by solving this type of flame. The look-up table is parametrized as a function of the mixture fraction z and the progress variable c. Finite rate chemistry modeling is employed for the progress variable source term closure,

while the GRI3.0 detailed mechanism is used for the table computation. This approach could be by taking into account the quenching effects of the flame front stretch and local heat losses. Regarding this, a modification of the FGM model through a dedicated correction was proposed by Klarmann et al. [15] in Reynolds Averaged Navier-Stokes (RANS) turbulence framework: this accounts for the reduced reactivity related to local distortion of the flame front and the subsequent alteration of the all diffusive process within the reaction layer and enhanced sensitivity to heat loss. Such effects are included by modifying the mean progress variable source term $\dot{\omega}_c$, that is the global reaction rate driving the turbulent flame propagation. The underlying strategy consists of applying a reduction factor Γ_k to $\dot{\omega}_c$, ranging between 0 and 1 to represent all the scenarios from the unmodified reaction rate to the local quenching. The reduction factor is evaluated at run-time with the following expression:

$$\Gamma_{\kappa,\psi} = \left(\frac{S_c(\kappa, \psi, z)}{S_c^{\,0}(z)}\right)^m \in [0,1]$$

Whereat the numerator is present the consumption speed related to the stretched and non-adiabatic flamelet for a given value of stretch κ, heat loss ψ, and mixture fraction z, while at the denominator the consumption speed referred to the same flamelet in un-stretched and adiabatic conditions. An exponential relation is present with a coefficient m which assumes a constant value considering the type of fuel and the operating conditions [15]. While $S_c^{\,0}$ is derived from the FGM look-up table, S_c is computed a priori as function of the mixture composition, strain, and heat loss levels and stored in an additional table. This latter tabulation is obtained from one-dimensional laminar flames considering a premixed counterflow configuration (i.e., fresh to equilibrium products as opposed jets) for this specific application thanks to the Cantera v2.4.0 libraries [16]. The values of stretch and the heat loss are computed directly in the CFD simulation, hence, together with the local composition, they are used to access the consumption speed look-up table. Since the use of LES turbulence modeling here, the original approach proposed by Klarmann has been adapted to the scale resolving context. The main differences are related to the strain computation, the introduction of the front curvature contribution on the flame stretch other than a different definition of heat loss. The reader interested in a complete description of the modifications for the LES context is addressed to the previous work by the authors [13]. It should be noticed that this procedure allows to include strain effects on the global reactivity avoiding the need for further control variables, but their impact on the flame structure tabulated in the manifold is neglected.

The last approach here adopted is the ATF model [17], which is instead based on a different strategy: the flame front is artificially thickened to directly solve the flame structure. This approach has been widely validated in literature for both premixed and non-premixed flames and nowadays is one of the most applied approaches for combustion modeling within unsteady simulations. Moreover, since the first introduction, new implementations able to avoid non-physical stretching of the flame through dynamic formulation, have been proposed in technical literature [18]. In the present work, the formulation available in the CFD solver ANSYS Fluent 2019-R1 is employed [11]. The main drawback of the ATF model is that often it is used together with reduced chemical mechanisms to mitigate the computational efforts required for the simulation. In the present work, the BFER 2 step mechanism developed by Franzelli [19] for air-methane mixture is employed.

Results
The numerical results are compared in this section with the available measurement from the experimental campaign by Fokaides. Regarding the reactive process, the main quantities of interest are the temperature field and carbon monoxide mole fraction, while velocity field measurements as well as local mixture composition help to understand the key features of this type of flame.
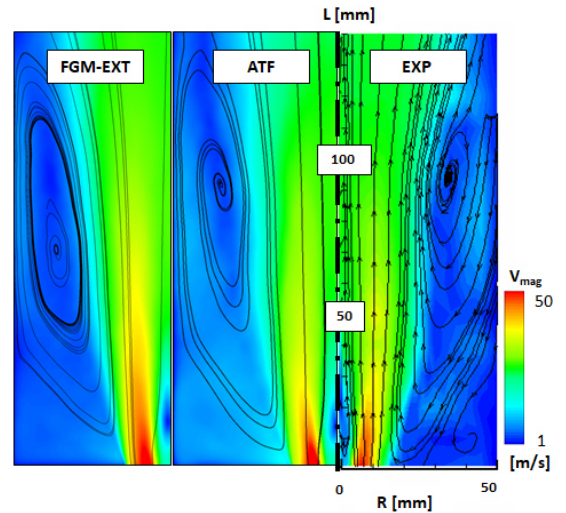

Figure 2 - Contour maps of velocity magnitude from FGM-EXT, ATF and experiments (from left to right) with flow-field streamlines superimposed.

In Figure 2 the velocity field on the midplane up to 175 mm is reported for both CFD and experiments in reactive conditions [4]. For the seek of brevity, only the results coming from the FGM-EXT and the ATF models, since the same outcome is observed in the case of the FGM. The results are in good agreement with the experimental data since all the key features of this nozzle concept can be observed: high-velocity streams are present close to the burner axis, rapidly decaying away from it in the radial direction. Also, it is visible the wide ORZ, extending from the burner dome deeply into the combustion chamber.
In the same manner, in Figure 3 the contour map of equivalence ratio from numerical simulations and experimental measurements are reported.

3

A good agreement is reached between experimental maps and numerical simulations regarding the composition in the combustion chamber: near the axis, the fresh mixture reaches higher values of equivalence ratio, then completing the mixing between air and fuel along with the LOH before reaching the flame front.
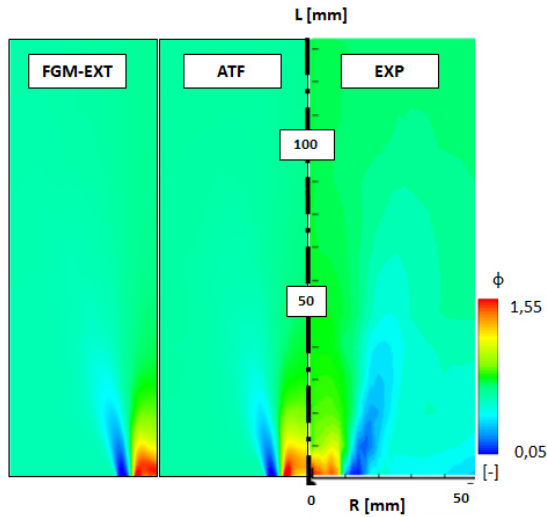

Figure 3 - Contour maps of equivalence ratio from FGM-EXT, ATF and experiments (from left to right) with flow-field streamlines superimposed

The lowest values of the equivalence ratio are reached at the nozzle exit due to the secondary swirler flow. The radial channels are indeed responsible for a flow characterized by a very lean mixture and high axial velocity. These flow structures act as a barrier between the recirculating hot gas and the fresh mixture in the inner region, preventing a flame reattachment.

The most significant comparison among the combustion models employed in this work is shown in Figure 4, where the contour maps of carbon monoxide mole fraction, X_{CO} are reported for all the combustion models and together with the experimental measurements. Each contour refers to the maximum value related to each simulation. This choice is mandatory to overcome the limits of the reduced chemistry employed for the ATF model, where X_{CO} assumes a value that is one order of magnitude lower than the ones from the detailed mechanism. Nevertheless, this comparison allows visualizing from a qualitative point of view the main reaction zone other than the flame shape and extension. Firstly, each combustion model is predicting the flame lift-off, since all the maps are showing the reaction zones detached from the nozzle exit: this fact was not trivial considering the results of the previous numerical work [7]. Considering the standard FGM model, the flame appears quite compact and short with respect to the experiments: the higher values of X_{CO} are showing an arrow-shaped flame according to the previous experimental findings [9], while the base of flame exhibits an anchoring edge placed side of the main swirling jet issuing from the nozzle. Moving to the FGM-EXT the prediction is improved since the flame extends more in the combustion chamber and it recovers a shape more similar to the experimental results. The inner region close to the burner axis now experiences a lowered reactivity due to the presence of an intense stretch field [13] through the introduced correction factor. As result, the main reaction zone is pushed downstream and stabilizes between 100 and 150 mm, which is not far from the experimental result. The flame base instead is still
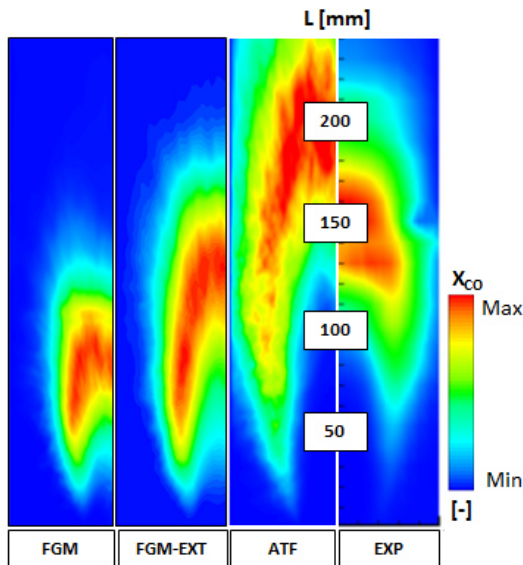

Figure 4 - Contour maps of averaged carbon monoxide mole fraction respectively for (from left to right) FGM, FGM-EXT, ATF combustion models, and xperimental data from [4].
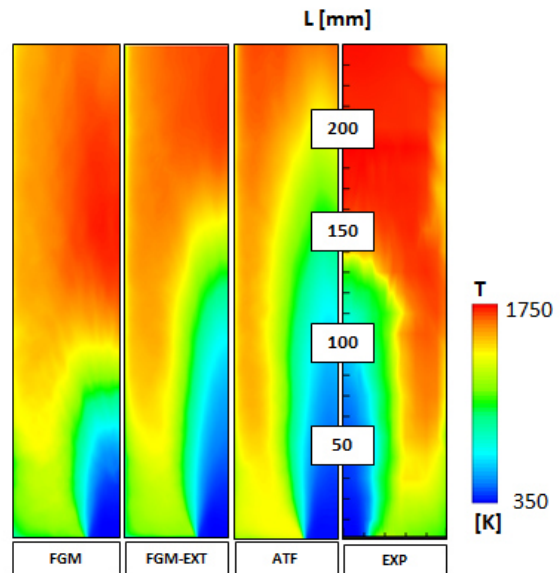

Figure 5 - Contour maps of averaged temperature respectively for (from left to right) FGM, FGM-EXT, ATF combustion models, and experimental data from [4].

4

anchored at the same height observed with the standard FGM model and generally high values of X_{CO} can be found in the shear layer between ORZ and the nozzle swirling jet.

Things change dramatically with the ATF model, where the main reaction zone is placed far away from the nozzle exit and even more downstream of the experimental

regarding the reaction zone is being obtained with the higher value of wall temperature, the temperature fields of both the FGM models are better representing the experimental maps near the bottom of the combustion chamber. Also, the region with the highest temperatures measured, close to the adiabatic flame temperature, seems better caught in terms of position by the FGM-
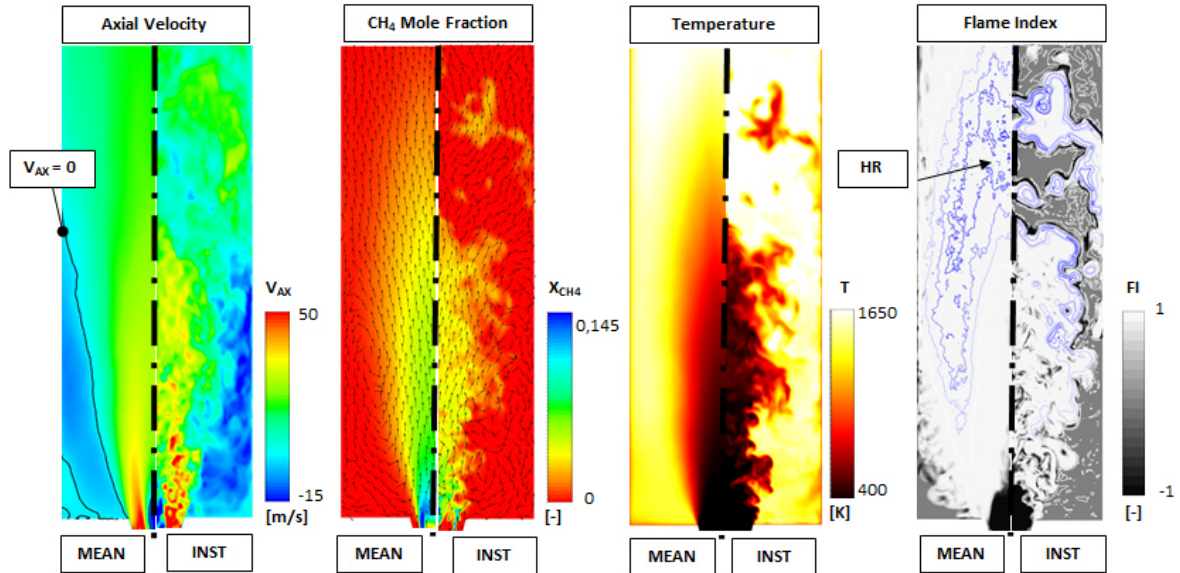

Figure 6 – Contour of mean and instantaneous of (from left to right) axial velocity, methane mole fraction, temperature, flame index with heat-release (HR) isolines superimposed. Normalized vectors of velocity are superimposed on the methane mole fraction map.

finding. The flame is still arrow-shaped, with an inner region free of reaction while the flame edge extends in the outer shear layer, similarly to the previous combustion models. Surprisingly, the flame base (considering the first regions where non-negligible values of X_{CO} are observed) is placed roughly at the same height as the other combustion models, when instead the experimental map shows a flame anchored beyond 50 mm. A possible explanation for this phenomenon could be pointed out by considering that autoignition of the fresh mixture promoted by the hot combustion products having a role in the flame edge position rather than a classic propagation of the flame front itself. In this fashion, the BFER mechanism is underestimating the autoignition time [20], therefore the flame seems to anchor at a low position in the combustion chamber. Meanwhile, the FGM model and the derived version employ a detailed mechanism able to reproduce correctly the autoignition time, but they are not taking into account properly the finite rate effects which delay the ignition and stabilized the flame downstream. This interesting fact will be the object of further investigation.

In Figure 5 the temperature field maps are reported again for all the combustion models and compared with the experimental results. In this case, less useful information can be retrieved due to the uncertainties related to the wall thermal boundary conditions. As mentioned, the FGM models and the ATF are employing different values of wall temperature: although the best prediction

EXT model rather than the ATF one. Apart from the value imposed to the wall boundary conditions, it is clear that a unique and uniform value of temperature applied to all the walls (i.e., entire combustion chamber and burner dome) is not correct and could have a relevant role in the flame representation.

In conclusion, the ATF model seems to better represent the flame, since by resolving the flame front it could describe the finite rate effects governing the whole process. Furthermore, all the experimental findings described in [3] seem to be reproduced. In Figure 6, the mean and instantaneous contour for the ATF simulation are reported in terms of the axial velocity field, methane mole fraction, temperature, and Flame Index, this latter according to the definition available in [21]:

$$FI = \frac{\nabla Y_{fuel} \cdot \nabla Y_{oxid}}{\left| \nabla Y_{fuel} \cdot \nabla Y_{oxid} \right|} \in [-1,1]$$

Such quantity indicates where the flame can be assumed in a premixed state or a non-premixed one. Isolines of zero axial velocity and heat release are superimposed respectively to the mean axial velocity contour map and the Flame Index one. As already observed, the flame stabilizes at a position where a sufficiently low value of the velocity is reached. This can be seen by both the presence of methane as well as the increase of mean temperature. The reaction is occurring in premixed-like conditions, as reported also in [3], as visible in the flame

index maps, since premixed conditions are reached very early in the combustion chamber. This fact confirms the potential of the lifted-flames with respect to the targets of this kind of application. Also, the temperature field instantaneous map shows the presence of flow instabilities at the base of the jet: this phenomenon leads to the entrainment of hot combustion products in the fresh mixture jet. This process operates a sort of continuous re-ignition of the mixture and it is reported in the literature as a further stabilization mechanism for this kind of flame [1].

Conclusions

The present work compares different combustion models within LES simulations to investigate a low-swirl partially premixed lifted flame employing gaseous fuel studied at KIT-EBI. The ATF and the FGM models are applied, together with a modified version of the second which includes a correction for the stretch and heat loss effects. The results are showing that the FGM approach overestimates the reactivity of the combustion process, resulting in flame stabilized too low in the combustion chamber. A better prediction can be reached when stretch and heat loss effects are included since the flame is elonged and closer to the experimental results. The best agreement is however obtained thanks to the ATF model in terms of the position of the main reaction zone. However, all the models exhibit an early occurrence of the reactive regions concerning the experimental data. In conclusion, the flamelet regime assumption seems not to be adequate to reproduce this type of flame. On the other hand, the reduced chemistry description employed with the ATF model could be responsible for a misprediction related to early ignition of the fresh mixture in the lower position of the flame tube. Future works will be focused on the influence of the chemistry description on this type of simulation.

Acknowledgments

References

[1] C. J. Lawn, *Prog. Energy Combust. Sci.*, vol. 35, no. 1, pp. 1–30, 2009.

[2] M. Day, S. Tachibana, J. Bell, M. Lijewski, V. Beckner, and R. K. Cheng, *Combust. Flame*, vol. 159, no. 1, pp. 275–290, 2012.

[3] P. A. Fokaides, P. Kasabov, and N. Zarzalis, *J. Eng. Gas Turbines Power*, vol. 130, no. 1, pp. 1–10, 2008.

[4] Fokaides, P.; Zarzalis, N. Lean blowout dynamics of a lifted stabilized, non-premixed swirl flame. Eur. Combust. Meet. 2007, 7, 2.

[5] P. Kasabov, N. Zarzalis, and P. Habisreuther, *Flow, Turbul. Combust.*, vol. 90, no. 3, pp. 605–619, 2013.

[6] K. M. Lyons, *Prog. Energy Combust. Sci.*, vol. 33, no. 2, pp. 211–231, 2007.

[7] Kern, M, Fokaides, P, Habisreuther, P, Zarzalis, N. *Proc. of the ASME Turbo Expo 2009: Power for Land, Sea, and Air. Volume 2: Combustion, Fuels and Emissions*. Orlando, Florida, USA. June 8–12, 2009. pp. 359-368. ASME.

[8] J. Sedlmaier, "Numerische und experimentelle Untersuchung einer abgehobenen Flamme unter Druck," 2019.

[9] P. A. Fokaides, P. Kasabov, and N. Zarzalis, *J. Eng. Gas Turbines Power*, vol. 130, no. 1, pp. 1–9, 2008.

[10] D. R. Lefebvre, Arthur H and Ballal, *Gas turbine combustion: alternative fuels and emissions*. CRC press, 2010.

[11] ANSYS Inc., *ANSYS Inc., USA*, vol. 15317, no. November, p. 814, 2013.

[12] D. K. Lilly, *Phys. Fluids*, vol. 4, no. 3, pp. 633–635, 1992.

[13] L. Langone, J. Sedlmaier, P. C. Nassini, L. Mazzei, S. Harth, and A. Andreini, *Proc. ASME Turbo Expo*, vol. 4B-2020, pp. 1–14, 2020.

[14] J. A. van Oijen, A. Donini, R. J. M. Bastiaans, J. H. M. ten Thije Boonkkamp, and L. P. H. de Goey, *Prog. Energy Combust. Sci.*, vol. 57, pp. 30–74, 2016.

[15] N. Klarmann, T. Sattelmayer, W. Geng, B. T. Zoller, and F. Magni, pp. 1–12, 2016.

[16] D. Goodwin, "Cantera: An object-oriented software toolkit for chemical kinetics, thermodynamics, and transport properties," 2018.

[17] O. Colin, F. Ducros, D. Veynante, and T. Poinsot, *Phys. Fluids*, vol. 12, no. 7, pp. 1843–1863, 2000.

[18] G. Wang, M. Boileau, and D. Veynante, *Combust. Flame*, vol. 158, no. 11, pp. 2199–2213, 2011.

[19] B. Franzelli, E. Riber, L. Y. M. Gicquel, and T. Poinsot, *Combust. Flame*, vol. 159, no. 2, pp. 621–637, 2012.

[20] C. Wang, C. Qian, J. Liu, and M. A. Liberman, *Combust. Flame*, vol. 197, pp. 400–415, 2018.

[21] D. A. Rosenberg, P. M. Allison, and J. F. Driscoll, *Combust. Flame*, vol. 162, no. 7, pp. 2808–2822, 2015.